

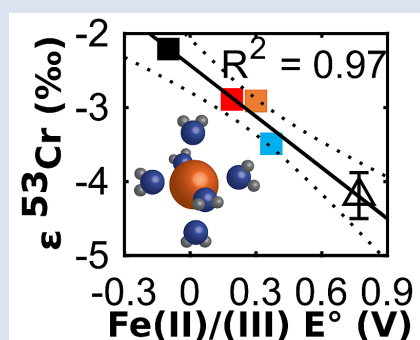
# Thermodynamic controls on redox-driven kinetic stable isotope fractionation

C. Joe-Wong<sup>1\*</sup>, K.L. Weaver<sup>2</sup>, S.T. Brown<sup>3</sup>, K. Maher<sup>2</sup>



doi:10.7185/geochemlet.1909

## Abstract



Stable isotope fractionation arising from redox reactions has the potential to illuminate the oxygenation of Earth's interior, oceans, and atmosphere. However, reconstruction of past and present redox conditions from stable isotope signatures is complicated by variable fractionations associated with different reduction pathways. Here we demonstrate a linear relationship between redox-driven kinetic fractionation and the standard free energy of reaction for aqueous chromium(VI) reduction by iron(II) species. We also show that the intrinsic kinetic fractionation factor is log-linearly correlated with the rate constant of reaction, which is in turn a function of the free energy of reaction. The linear free energy relationship for kinetic fractionation describes both our experimental results and previous observations of chromium isotope fractionation and allows the magnitude of fractionation to be directly linked to environmental conditions such as pH and oxygen levels. By demonstrating that the magnitude of kinetic fractionation can be thermodynamically controlled, this study systematically explains the large variability in chromium(VI) isotope fractionation and provides a conceptual framework that is likely applicable to other isotope systems.

Received 30 October 2018 | Accepted 26 February 2019 | Published 29 March 2019

## Introduction

Stable isotope fractionation is used to examine Earth processes ranging from the evolution of redox conditions in ancient oceans (Frei *et al.*, 2009) to the fate of modern contaminant plumes (Ellis *et al.*, 2002). Interpreting the isotopic signatures observed in these systems requires frameworks to link fractionation to environmental variables. For instance, fractionation during precipitation can be modelled as a function of solvation energies and the composition of ions in solution or the balance between forward and backward reaction rates (Fantle and DePaolo, 2007; DePaolo, 2011; Hofmann *et al.*, 2012; Nielsen *et al.*, 2012). Similarly, Kavner and colleagues have shown that kinetic fractionation during metal electroplating scales linearly with the standard electrode potential ( $E^\circ$ ) (Kavner *et al.*, 2005, 2008). However, if the standard electrode potential is taken to be analogous to the free energy of reaction ( $\Delta G_r^\circ$ ) in natural soils and sediments, this relationship has not yet been demonstrated for non-electrochemical reactions.

Knowledge of the thermodynamic controls on kinetic fractionation could be used to interpret redox-driven isotope fractionation in natural systems. The relationship between thermodynamic parameters ( $E^\circ$  or  $\Delta G_r^\circ$ ) and the kinetics of electron transfer can be formalised *via* Marcus theory (Marcus,

1964, 1965, 1993). Unlike other models that link changes in observed fractionation with shifts between kinetic and equilibrium fractionation (DePaolo, 2011), Marcus theory predicts changes in the kinetic fractionation factor itself. For most electron transfer reactions, Marcus theory predicts that the rate constant ( $k$ ) should increase log-linearly as  $\Delta G_r^\circ$  decreases, such that a reaction that is more thermodynamically favourable in the standard state is faster. Kavner and colleagues have shown that Marcus theory also describes kinetic isotope fractionation during redox reactions (Kavner *et al.*, 2005, 2008). Specifically, Marcus theory predicts that the kinetic fractionation factor ( $\epsilon_{kin}$ ) follows a linear free energy relationship for redox reactions with similar reaction mechanisms and equilibrium fractionation factors. A reaction with a lower  $\Delta G_r^\circ$  has a lower activation energy, and the difference between the activation energies of different isotopologues is also smaller. Thus, a redox reaction that is more thermodynamically favourable in the standard state is not only faster but also exhibits less kinetic fractionation.

For isotope fractionation in natural systems, the combination of electron donor and acceptor determines  $\Delta G_r^\circ$ . For example, as an oxidant such as Cr(VI) enters an aquifer and travels along a flow path characterised by decreasing  $O_2$  and  $E_h$ , Cr(VI) also encounters a changing series of abiotic reductants, *e.g.*, from trace Fe(II) sorbed onto goethite to aqueous

1. Department of Geological Sciences, Stanford University, 450 Serra Mall, Building 320, Stanford, CA 94305, USA  
2. Department of Earth System Science, Stanford University, 473 Via Ortega, Stanford, CA 94305, USA  
3. Energy Geosciences Division, Lawrence Berkeley National Laboratory, 1 Cyclotron Road, Berkeley, CA 94720, USA  
\* Corresponding author (email: joewongc@stanford.edu)



Fe(II) to Fe(II) sulphides, in broad accordance with the redox ladder (Champ *et al.*, 1979). This sequence of reductants results in a shifting  $\Delta G_r^\circ$  for the reduction of Cr(VI). If  $\Delta G_r^\circ$  also influences  $k$  and  $\epsilon_{kin}$ , we would expect kinetic isotope fractionation during Cr(VI) reduction to change along the flow path in a predictable fashion, consistent with electrochemical experiments. To date, the expected linear relationship between  $\epsilon_{kin}$  and  $\Delta G_r^\circ$  has not been demonstrated in natural systems.

To test for a thermodynamic control on kinetic fractionation, we examined a model system, Cr(VI) reduction by aqueous Fe(II). Chromium(VI) reduction was chosen because it consistently results in kinetic isotope fractionation (Wang *et al.*, 2015) and is actively cycled in aquifers and marine sediments, even though the multi-electron reduction is more difficult to model explicitly. Chromium naturally occurs as Cr(VI), which is generally soluble and toxic, and as Cr(III), which is both far less soluble and environmentally benign (Ball and Nordstrom, 1998). Fractionation during Cr(VI) reduction induces kinetic fractionation that enriches the remaining Cr(VI) in the heavier isotopes (Ellis *et al.*, 2002). This fractionation may be documented as positive isotopic excursions in the rock record (Ellis *et al.*, 2002; Frei *et al.*, 2009). In modern environments, Cr(VI) isotope signatures may fingerprint reduction of Cr(VI) pollution (Berna *et al.*, 2010).

The unexplained variability in  $\epsilon_{kin}$  for Cr(VI) reduction, which ranges from -0.2 ‰ to -5 ‰, poses a barrier to interpretation of Cr isotope signatures (Qin and Wang, 2017). Although faster reduction often causes less fractionation of Cr(VI) (Sikora *et al.*, 2008; Basu and Johnson, 2012; Jamieson-Hanes *et al.*, 2014), the origin of this effect has not been established. In accordance with predictions from electrochemical experiments, we demonstrate a log-linear relationship between  $\epsilon_{kin}$  and  $k$  for Cr(VI) reduction by aqueous Fe(II) that arises from the dependence of both  $\epsilon_{kin}$  and  $k$  on  $\Delta G_r^\circ$ . Aqueous Fe(II) is one of the fastest naturally occurring reductants of Cr(VI) at circumneutral pH (Fendorf *et al.*, 2000), but hydrolysis and organic ligation of Fe(II) alter its standard reduction potential ( $E^\circ$ ) such that the rate constant of Cr(VI) reduction varies by orders of magnitude, depending on the speciation of Fe(II) (Buerge and Hug, 1997, 1998). It has not been established whether changes in  $\epsilon_{kin}$  are associated with these changes in  $k$  because fractionation during Cr(VI) reduction by aqueous Fe(II) has only been explored in a narrow pH range (Kitchen *et al.*, 2012). By changing the ligation of Fe(II), we show experimentally and theoretically that the variation in the Cr kinetic fractionation factor can be explained in terms of a linear free energy relationship.

## Results

Isotope fractionation of Cr(VI) was measured during the step-wise batch reduction of Cr(VI) by Fe(II)-citrate, Fe(II)-nitrioltriacetate, and Fe(II)-salicylate at pH 5.5 and by aqueous Fe(II) at pH values ranging from 5.0 to 7.3, following the method of Kitchen *et al.* (2012). Experimental details are available in the Supplementary Information (Methods section and Table S-1). The remaining Cr(VI) was progressively enriched in heavier isotopes for all experiments. Both organic ligation of Fe(II) (Table S-2) and pH (Table S-3) affect the extent of fractionation. The observed Cr isotope fractionation can be described using a Rayleigh distillation model with a single fractionation factor ( $\epsilon = \alpha - 1$ , expressed in per mille) for each experiment (Figs. 1, S-1). Every experiment was carried out in duplicate, and no duplicates show major differences from each other.

Measured fractionation factors range from -1.7 to -3.5 ‰. The 2 ‰ range nearly spans the range of all reported fractionation factors for naturally occurring abiotic reductants of Cr(VI) (Jamieson-Hanes *et al.*, 2014). All fractionation factors are smaller than equilibrium fractionation between inorganic Cr(VI) and Cr(III) species (-6 to -7 ‰), which is unlikely to have been approached within the experimental timescale (Schauble *et al.*, 2004; Wang *et al.*, 2015), as discussed further in the Supplementary Information. All fractionation is therefore assumed to be kinetic.

Fractionation factors for Cr(VI) reduction are strongly correlated with  $E^\circ$  of the Fe(II)-Fe(III) half-reaction, which is a proxy for  $\Delta G_r^\circ$  of the electron transfers between Fe(II) and Cr(VI) (Fig. 2a). For Cr(VI) reduction by an Fe(II) species with a low  $E^\circ$ , for which the oxidation of Fe(II) and concomitant reduction of Cr(VI) are thermodynamically favourable, the magnitude of  $\epsilon$  is small. Furthermore,  $\epsilon$  is also linearly correlated with  $\log(k)$ , whereby a faster reaction induces less fractionation (Fig. 2b). This correlation, which is consistent with previous qualitative observations (Sikora *et al.*, 2008; Basu and Johnson, 2012; Jamieson-Hanes *et al.*, 2014), is unlikely to be caused by transport limitations in the vigorously stirred reactors (see Supplementary Information). Instead, the correlation between  $\epsilon$  and  $\log(k)$  is likely a by-product of the dependence of both variables on  $E^\circ$  of the Fe(II)-Fe(III) half-reaction (Buerge and Hug, 1997, 1998). The correlations between  $\epsilon$ ,  $\log(k)$ , and  $E^\circ$  are consistent with Marcus theory and previous electrochemical observations (Kavner *et al.*, 2005, 2008).

## Environmental Applications

The systematic influence of  $\Delta G_r^\circ$  on  $\epsilon$  may be used to relate isotopic effects to environmental conditions such as the abundance of organic matter and pH. For example, organic ligation of aqueous Fe(II) is significant in marine systems and many subsurface environments (Jansen *et al.*, 2003; Morel and Price, 2003). Our results show that organic ligation of Fe(II) strongly affects isotope fractionation during reduction of Cr(VI) and potentially other redox partners. Similarly, fractionation during Cr(VI) reduction by aqueous inorganic Fe(II) depends on pH. Expanding the pH range of a previous study, we find that the effective fractionation factor ( $\epsilon_{eff}$ ) for Cr(VI) reduction by Fe(II) decreases in magnitude from -4.2 ‰ at pH 4.0 (Kitchen *et al.*, 2012) to -2.2 ‰ at pH 7.3 (Figs. 1, S-1; Table S-3).

The pH dependence of  $\epsilon_{eff}$  is caused by the shift in the effective reductant of Cr(VI) with pH. Three Fe(II) species reduce Cr(VI) under the reaction conditions:  $\text{Fe}(\text{H}_2\text{O})_6^{2+}$ ,  $\text{FeOH}^+$ , and  $\text{Fe}(\text{OH})_2^0$ . Although the vast majority of Fe(II) is present as  $\text{Fe}(\text{H}_2\text{O})_6^{2+}$  for all tested pH values, the concentrations of the two hydrolysed species increase as pH increases. Because hydrolysis lowers  $E^\circ$  of the Fe(II)-Fe(III) half-reaction, making Fe(II) more susceptible to oxidation,  $\text{FeOH}^+$  and  $\text{Fe}(\text{OH})_2^0$  are more thermodynamically favourable and hence faster reductants of Cr(VI) (Buerge and Hug, 1997; Pettine *et al.*, 1998). Thus, as pH increases,  $\text{FeOH}^+$  and  $\text{Fe}(\text{OH})_2^0$  become the dominant reductants of Cr(VI) in turn (Fig. 3a). The fraction of Cr(VI) reduced by each species in the environmentally relevant pH range of 4-7 was quantified using two species-specific rate laws from Pettine *et al.* (1998) and Buerge and Hug (1997). Although the overall rates predicted by these models are broadly consistent, the contribution of each Fe(II) species differs.

We modelled the pH dependence of  $\epsilon_{eff}$  using the linear free energy relationship described above by conceptualising  $\epsilon_{eff}$  as the average of the fractionation factors for Cr(VI) reduction

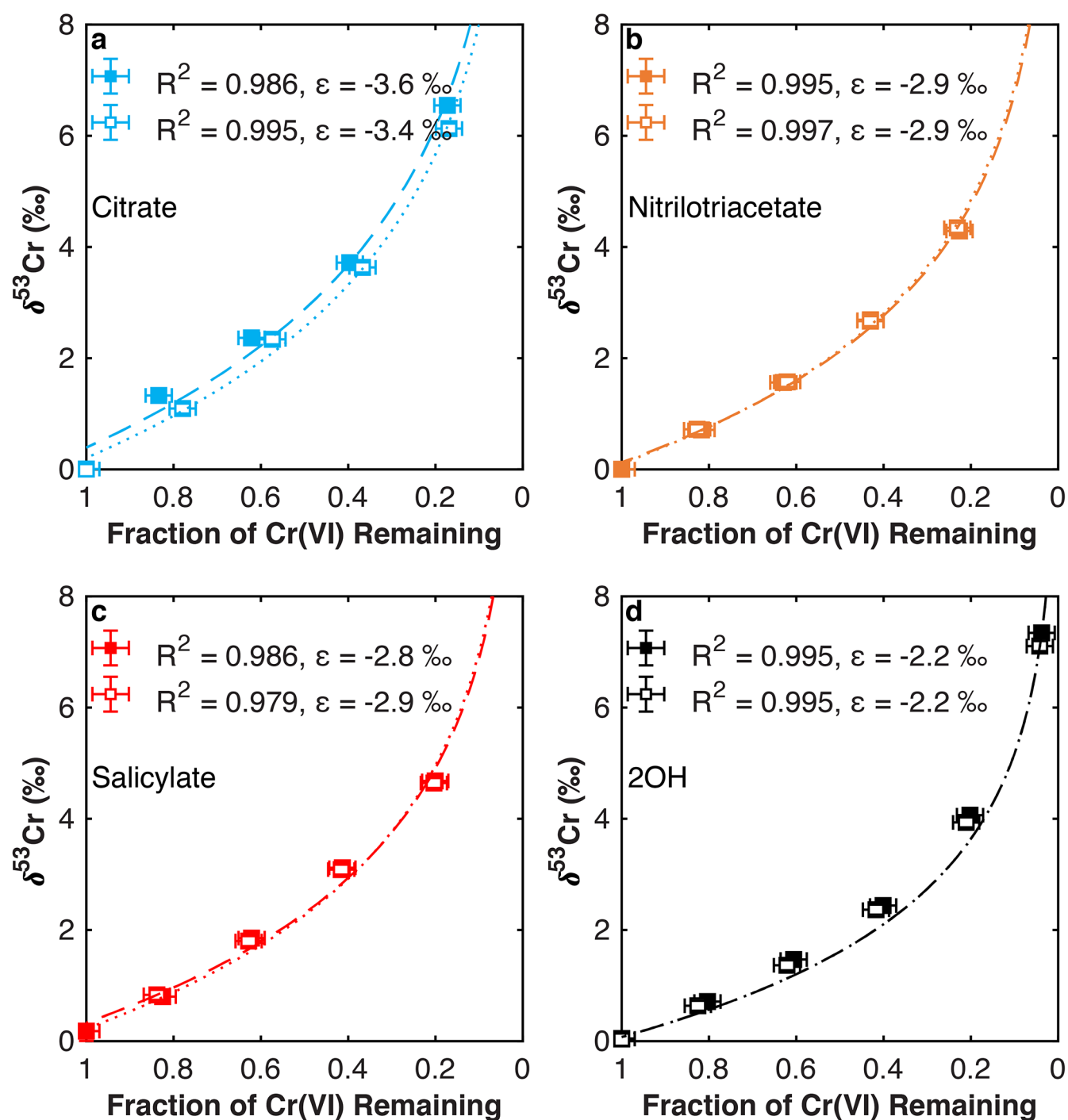


**Figure 1** Isotope fractionation during Cr(VI) reduction by various aqueous Fe(II) species. Filled and open symbols in each plot show duplicate reactors. Rayleigh curves based on linear best fits are plotted as dashed lines (filled symbols) and dotted lines (open symbols). Vertical error bars (2 s.d.) are smaller than the symbols.

by each Fe(II) species (*i.e.*  $\text{Fe}(\text{H}_2\text{O})_6^{2+}$ ,  $\text{FeOH}^+$ , and  $\text{Fe}(\text{OH})_2^0$ ), weighted by the fraction of Cr(VI) reduced by each species. The linear free energy relationship allows the fractionation factor for  $\text{FeOH}^+$  to be interpolated ( $\epsilon_{\text{OH}} = -3.2$  ‰), and interpolated fractionation factors for  $\text{Fe}(\text{H}_2\text{O})_6^{2+}$  and  $\text{Fe}(\text{OH})_2^0$  are indistinguishable from the measured values. Because the two rate laws predict different contributions of each Fe(II) species to the overall reduction of Cr(VI) within the studied pH range, the models also predict different trends in  $\epsilon_{\text{eff}}$  (Fig. 3b). Although neither model fits the data exactly, the model based on the rate law of Pettine *et al.* (1998) reproduces the general shape and trend of the data far better. Discrepancies are likely due to the uncertainties for the species-specific rate constants (Fig. S-2). Isotope fractionation thus offers a second axis on which to

evaluate otherwise indistinguishable rate laws and improve modelling of aqueous reduction kinetics.

Our results demonstrate a systematic relationship between  $\epsilon_{\text{kin}}$ ,  $k$ , and  $\Delta G_r^\circ$  as predicted by Marcus theory. This relationship may give rise to variable kinetic isotope effects along natural redox gradients. As conditions become more reducing and different reductants become available,  $\Delta G_r^\circ$  of Cr(VI) reduction decreases, resulting in a corresponding decrease in the magnitude of kinetic fractionation (Fig. 4). We observed this quantitatively for Cr(VI) reduction by aqueous Fe(II) species (Fig. 2) and show here that the values for a more diverse set of representative reductants are broadly consistent with the predicted trend (Ellis *et al.*, 2002;

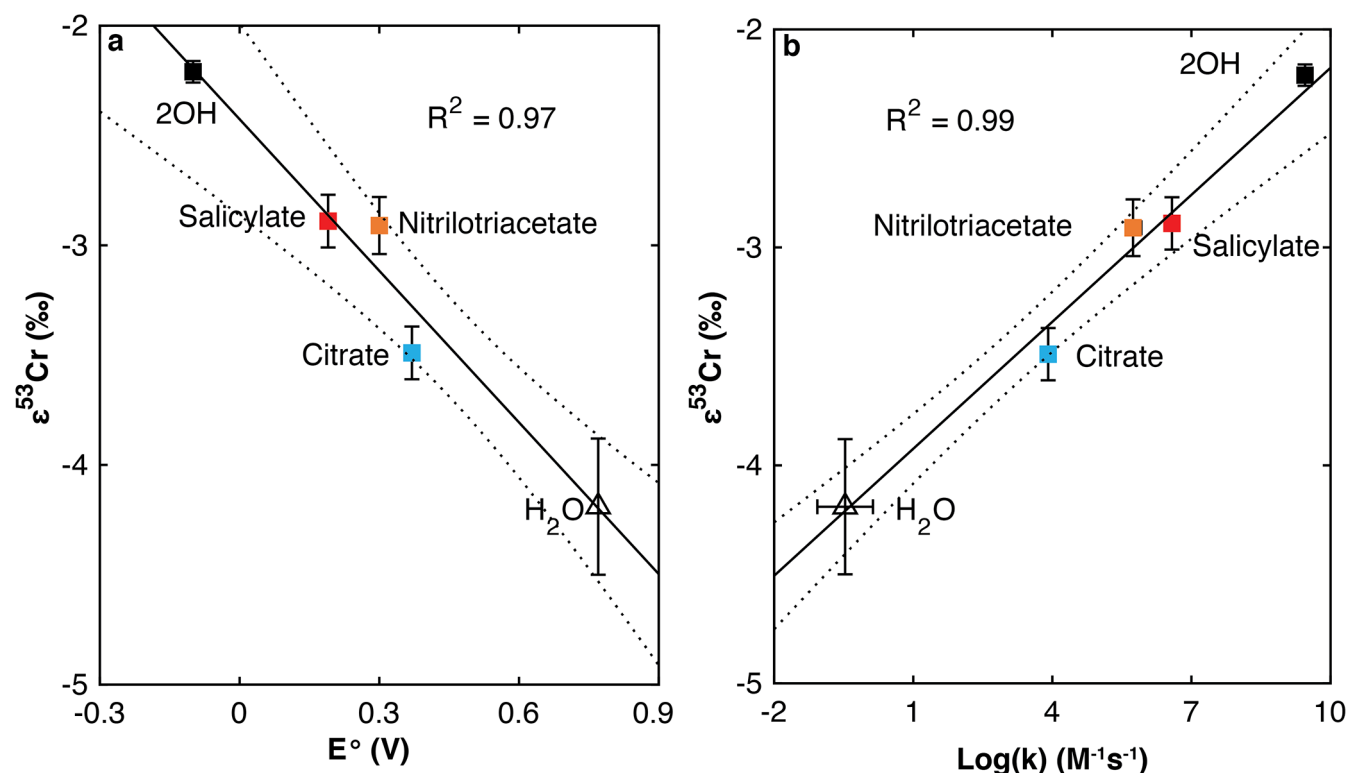


**Figure 2** Linear relationships of kinetic isotope fractionation factor for Cr(VI) reduction with (a) the Fe(II)-Fe(III) standard reduction potential and (b) rate constants. Solid line shows weighted linear regression, and dotted lines show 95 % confidence interval. Each symbol shows the average fractionation factor calculated for replicate experiments. Error bars are 2 s.d. The fractionation factor for Cr(VI) reduction by  $\text{Fe}(\text{H}_2\text{O})_6^{2+}$  is taken from Kitchen *et al.* (2012), and the rate constants are taken from Buerge and Hug (1997, 1998).

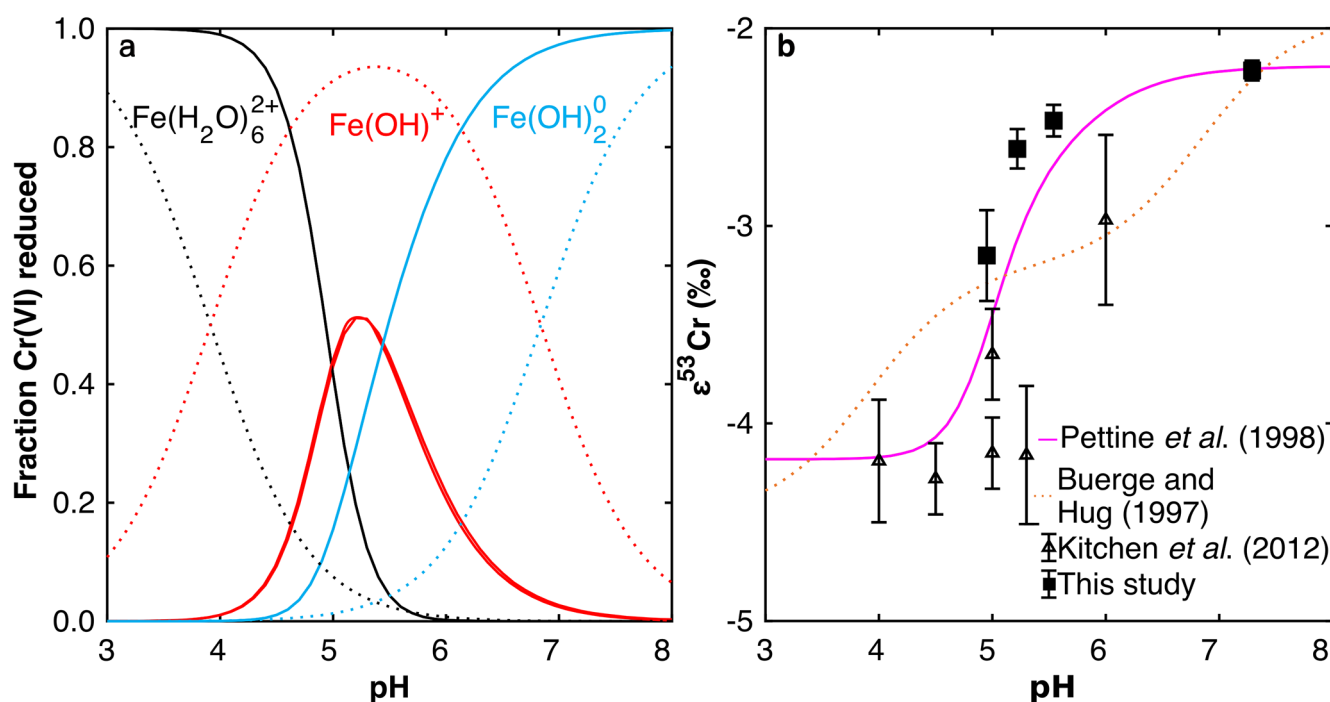


**Figure 3** Effects of pH on the kinetics and isotope fractionation of Cr(VI) reduction by aqueous Fe(II). In both parts, solid lines show the model based on the rate law of Pettine *et al.* (1998); dashed lines show the model based on the rate law of Buerge and Hug (1997). (a) The fraction of Cr(VI) reduced by each Fe(II) species is contingent on pH-dependent Fe(II) speciation and the rate law of Cr(VI) reduction. (b) The effective fractionation factor is the weighted average of the fractionation factors for Cr(VI) reduction by each Fe(II) species. Error bars on the symbols in (b) are 2 s.d.



Basu and Johnson, 2012; Kitchen *et al.*, 2012). Thermodynamically driven kinetic isotope effects thus explain part of the scatter in observed fractionation factors. Ultimately, predictable changes in Cr kinetic fractionation along redox gradients may help to distinguish between anoxic and euxinic palaeo-redox conditions and allow first order estimates of Cr(VI) fractionation in natural settings.

High O<sub>2</sub> /  
Young water

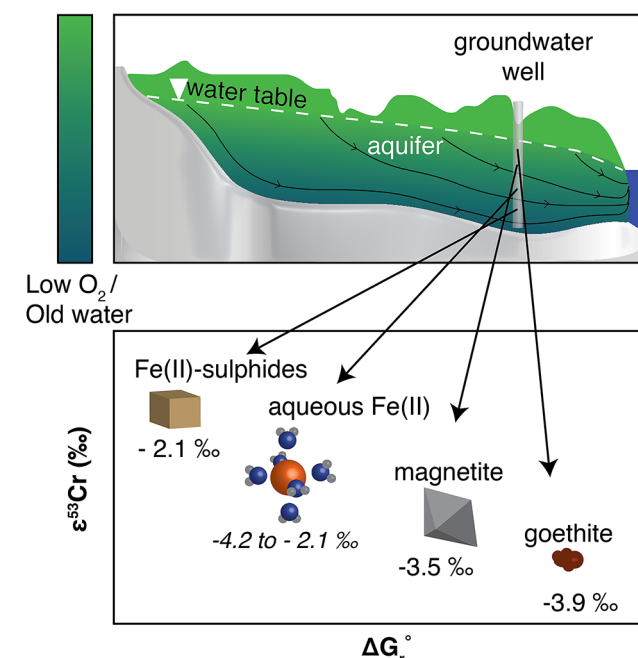


**Figure 4** Schematic of Cr(VI) reduction and variations in  $\epsilon_{kin}$  with depth, groundwater age, and oxygen levels. The dominant reductants are ordered according to their relative locations on the redox tower. Kinetic fractionation factors are taken from this study; aqueous Fe(II); Kitchen *et al.* (2012), aqueous Fe(II); Basu and Johnson (2012), Fe(II)-doped goethite and Fe(II) sulphide, and Ellis *et al.* (2002), magnetite.

## Conclusions

Fundamental understanding of redox-driven kinetic fractionation will strengthen our ability to interpret environmental change, especially along redox gradients. Capturing redox-dependent kinetic isotope effects may be aided by using linear free energy relationships to interpolate fractionation factors from limited experimental data. More research is needed to evaluate the applicability of Marcus theory to other stable isotope systems, particularly during oxidation and for more complex, heterogeneous and microbially mediated redox reactions. Fractionation during Cr(VI) reduction is generally solely kinetic (Qin and Wang, 2017), so the predicted linear free energy relationship observed herein is unambiguous. In other redox-driven systems that approach isotopic equilibrium, the relationship between observed fractionation and  $\Delta G_r^\circ$  is likely more complicated. Predicting observed fractionation in these cases may require combining Marcus theory with a model that predicts the shift between kinetic and equilibrium fractionation such as that in DePaolo (2011). Combining Marcus theory with other models would also be necessary if a significant component of fractionation is not redox-driven. Nevertheless, similar trends should exist for other redox-sensitive elements; metals such as U exhibit significant fractionation upon reduction (Brown *et al.*, 2018), and traditional light

stable isotope systems also may be described by linear free energy relationships (Gorski *et al.*, 2010). By permitting more precise interpretations of redox-driven isotope fractionation, the framework presented here is poised to improve our understanding of redox dynamics.

## Acknowledgements

This work was supported by a National Science Foundation Career Award (EAR-1254156) to KM. CJ.-W was funded by the United States Department of Defense through a National Defense Science & Engineering Graduate Fellowship and by a Stanford Graduate Fellowship. STB. was funded by the U.S. Department of Energy, Office of Basic Energy Sciences (DE-AC02-05CH11231).

Editor: Liane G. Benning

## Additional Information

**Supplementary Information** accompanies this letter at <http://www.geochemicalperspectivesletters.org/article1909>.



This work is distributed under the Creative Commons Attribution Non-Commercial No-Derivatives 4.0 License, which permits unrestricted distribution provided the original author and source are credited. The material may not be adapted (remixed, transformed or built upon) or used for commercial purposes without written permission from the author. Additional information is available at <http://www.geochemicalperspectivesletters.org/copyright-and-permissions>.

**Cite this letter as:** Joe-Wong, C., Weaver, K.L., Brown, S.T., Maher, K. (2019) Thermodynamic controls on redox-driven kinetic stable isotope fractionation. *Geochem. Persp. Let.* 10, 20–25.

## References

- BALL, J.W., NORDSTROM, D.K. (1998) Critical Evaluation and Selection of Standard State Thermodynamic Properties for Chromium Metal and Its Aqueous Ions, Hydrolysis Species, Oxides, and Hydroxides. *Journal of Chemical & Engineering Data* 43, 895–918.
- BASU, A., JOHNSON, T.M. (2012) Determination of Hexavalent Chromium Reduction Using Cr Stable Isotopes: Isotopic Fractionation Factors for Permeable Reactive Barrier Materials. *Environmental Science & Technology* 46, 5353–5360.
- BERNA, E.C., JOHNSON, T.M., MAKDISI, R.S., BASU, A. (2010) Cr Stable Isotopes As Indicators of Cr(VI) Reduction in Groundwater: A Detailed Time-Series Study of a Point-Source Plume. *Environmental Science & Technology* 44, 1043–1048.
- BROWN, S.T., BASU, A., DING, X., CHRISTENSEN, J.N., DEPAOLO, D.J. (2018) Uranium isotope fractionation by abiotic reductive precipitation. *Proceedings of the National Academy of Sciences* 201805234.
- BUERGE, I.J., HUG, S.J. (1997) Kinetics and pH Dependence of Chromium(VI) Reduction by Iron(II). *Environmental Science & Technology* 31, 1426–1432.
- BUERGE, I.J., HUG, S.J. (1998) Influence of Organic Ligands on Chromium(VI) Reduction by Iron(II). *Environmental Science & Technology* 32, 2092–2099.
- CHAMP, D.R., GULENS, J., JACKSON, R.E. (1979) Oxidation–reduction sequences in ground water flow systems. *Canadian Journal of Earth Sciences* 16, 12–23.
- DEPAOLO, D.J. (2011) Surface kinetic model for isotopic and trace element fractionation during precipitation of calcite from aqueous solutions. *Geochimica et Cosmochimica Acta* 75, 1039–1056.
- ELLIS, A.S., JOHNSON, T.M., BULLEN, T.D. (2002) Chromium Isotopes and the Fate of Hexavalent Chromium in the Environment. *Science* 295, 2060–2062.

- FANTLE, M.S., DEPAOLO, D.J. (2007) Ca isotopes in carbonate sediment and pore fluid from ODP Site 807A: The  $\text{Ca}^{2+}(\text{aq})$ -calcite equilibrium fractionation factor and calcite recrystallization rates in Pleistocene sediments. *Geochimica et Cosmochimica Acta* 71, 2524–2546.
- FENDORF, S., WIELINGA, B.W., HANSEL, C.M. (2000) Chromium Transformations in Natural Environments: The Role of Biological and Abiological Processes in Chromium(VI) Reduction. *International Geology Review* 42, 691–701.
- FREI, R., GAUCHER, C., POULTON, S.W., CANFIELD, D.E. (2009) Fluctuations in Precambrian atmospheric oxygenation recorded by chromium isotopes. *Nature* 461, 250–253.
- GORSKI, C.A., NURMI, J.T., TRATNYEK, P.G., HOFSTETTER, T.B., SCHERER, M.M. (2010) Redox Behavior of Magnetite: Implications for Contaminant Reduction. *Environmental Science & Technology* 44, 55–60.
- HOFMANN, A.E., BOURG, I.C., DEPAOLO, D.J. (2012) Ion desolvation as a mechanism for kinetic isotope fractionation in aqueous systems. *Proceedings of the National Academy of Sciences* 109, 18689–18694.
- JAMIESON-HANES, J.H., LENTZ, A.M., AMOS, R.T., PTACEK, C.J., BLOWES, D.W. (2014) Examination of Cr(VI) treatment by zero-valent iron using in situ, real-time X-ray absorption spectroscopy and Cr isotope measurements. *Geochimica et Cosmochimica Acta* 142, 299–313.
- JANSEN, B., NIEROP, K.G.J., VERSTRATEN, J.M. (2003) Mobility of Fe(II), Fe(III) and Al in acidic forest soils mediated by dissolved organic matter: influence of solution pH and metal/organic carbon ratios. *Geoderma* 113, 323–340.
- KAVNER, A., BONET, F., SHAHAR, A., SIMON, J., YOUNG, E. (2005) The isotopic effects of electron transfer: An explanation for Fe isotope fractionation in nature. *Geochimica et Cosmochimica Acta* 69, 2971–2979.
- KAVNER, A., JOHN, S.G., SASS, S., BOYLE, E.A. (2008) Redox-driven stable isotope fractionation in transition metals: Application to Zn electroplating. *Geochimica et Cosmochimica Acta* 72, 1731–1741.
- KITCHEN, J.W., JOHNSON, T.M., BULLEN, T.D., ZHU, J., RADDATZ, A. (2012) Chromium isotope fractionation factors for reduction of Cr(VI) by aqueous Fe(II) and organic molecules. *Geochimica et Cosmochimica Acta* 89, 190–201.
- MARCUS, R.A. (1964) Chemical and electrochemical electron-transfer theory. *Annual Review of Physical Chemistry* 15, 155–196.
- MARCUS, R.A. (1965) On the Theory of Electron-Transfer Reactions. VI. Unified Treatment for Homogeneous and Electrode Reactions. *The Journal of Chemical Physics* 43, 679–701.
- MARCUS, R.A. (1993) Electron transfer reactions in chemistry. Theory and experiment. *Reviews of Modern Physics* 65, 599–610.
- MOREL, F.M.M., PRICE, N.M. (2003) The Biogeochemical Cycles of Trace Metals in the Oceans. *Science* 300, 944–947.
- NIELSEN, L.C., DEPAOLO, D.J., DE YOREO, J.J. (2012) Self-consistent ion-by-ion growth model for kinetic isotopic fractionation during calcite precipitation. *Geochimica et Cosmochimica Acta* 86, 166–181.
- PETTINE, M., D'OTTONE, L., CAMPANELLA, L., MILLERO, F.J., PASSINO, R. (1998) The reduction of chromium (VI) by iron (II) in aqueous solutions. *Geochimica et Cosmochimica Acta* 62, 1509–1519.
- QIN, L., WANG, X. (2017) Chromium Isotope Geochemistry. *Reviews in Mineralogy and Geochemistry* 82, 379–414.
- SCHAUBLE, E., ROSSMAN, G.R., TAYLOR JR., H.P. (2004) Theoretical estimates of equilibrium chromium-isotope fractionations. *Chemical Geology* 205, 99–114.
- SIKORA, E.R., JOHNSON, T.M., BULLEN, T.D. (2008) Microbial mass-dependent fractionation of chromium isotopes. *Geochimica et Cosmochimica Acta* 72, 3631–3641.
- WANG, X., JOHNSON, T.M., ELLIS, A.S. (2015) Equilibrium isotopic fractionation and isotopic exchange kinetics between Cr(III) and Cr(VI). *Geochimica et Cosmochimica Acta* 153, 72–90.